

# Generating multi-scroll chaotic attractors by thresholding

Jinhu Lü<sup>a,\*</sup>, K. Murali<sup>b</sup>, Sudeshna Sinha<sup>c</sup>, Henry Leung<sup>d</sup>, M.A. Aziz-Alaoui<sup>e</sup>

<sup>a</sup> *Institute of Systems Science, Academy of Mathematics and Systems Science, Chinese Academy of Sciences, Beijing 100080, China*

<sup>b</sup> *Department of Physics, Anna University, Chennai 600 025, India*

<sup>c</sup> *Institute of Mathematical Sciences, Taramani, Chennai 600 113, India*

<sup>d</sup> *Department of Electrical and Computer Engineering, University of Calgary, Calgary, Canada T2N 1N4*

<sup>e</sup> *Applied Mathematics Laboratory, University of Le Havre, BP 540, 76058 Le Havre Cedex, France*

Received 17 September 2007; received in revised form 7 January 2008; accepted 30 January 2008

Available online 5 February 2008

Communicated by A.R. Bishop

## Abstract

This Letter proposes a novel thresholding approach for creating multi-scroll chaotic attractors. The general jerk circuit and Chua's circuit with sine nonlinearity are then used as two representative examples to show the working principle of this method. The controlled jerk circuit can generate various limit cycles and multi-scroll chaotic attractors by tuning the thresholds and the width of inner threshold plateau. The dynamic mechanism of threshold control is further explored by analyzing the system dynamical behaviors. In particular, this approach is effective and easy to be implemented since we only need to monitor the threshold variables or their functions and then reset them if they exceed the desired thresholds. Furthermore, two simple block circuit diagrams with threshold controllers are designed for the implementations of 1, 2, 3-scroll chaotic attractors. It indicates the potential engineering applications for various chaos-based information systems.

© 2008 Elsevier B.V. All rights reserved.

**Keywords:** Multi-scroll chaotic attractors; Circuit implementation; Switching control

## 1. Introduction

Over the past two decades, chaos control has seen a dramatic increase since chaos is useful and has great potential in many real-world engineering fields such as biomedical engineering, digital data encryption, power systems protection, reconfigurable hardware, and so on [1–3].

In essence, chaos control is guiding a chaotic system to reach a desired goal dynamics via various controllers. Recently, many different approaches or techniques have been proposed to achieve chaos control, such as OGY approach, linear feedback control, inverse optimal control, among many others [1–5]. It is well known that the theoretical basis of most known methods is stabilizing the unstable periodic orbits via parameter perturbation [3–5]. However, in this Letter, we introduce a novel threshold control approach, which clips the desired state vari-

ables or their functions instead of tuning system parameters, to realize a contrary goal for creating complex multi-scroll chaotic attractors [6–21].

There have been a large number of publications devoted to the research topic of circuit design for generating multi-scroll chaotic attractors over the last two decades [6–21]. Suykens and Vandewalle introduced a family of  $n$ -double scroll chaotic attractors [6]. Lü et al. proposed a switching manifold approach for creating chaotic attractors with multiple-merged basins of attraction [7,8]. Yalcin et al. presented a family of scroll grid attractors by using a step function approach [16], including one-dimensional (1-D)  $n$ -scroll, two-dimensional (2-D)  $(n \times m)$ -grid scroll, and three-dimensional (3-D)  $(n \times m \times l)$ -grid scroll chaotic attractors. Lü et al. proposed the hysteresis series and saturated series methods for generating 1-D  $n$ -scroll, 2-D  $(n \times m)$ -grid scroll, and 3-D  $(n \times m \times l)$ -grid scroll chaotic attractors with rigorous theoretical proofs and experimental verifications [10,12,13].

In general, compared with the single-scroll chaotic attractors, the multi-scroll chaotic attractors have much higher com-

\* Corresponding author.

E-mail addresses: [jhlu@iss.ac.cn](mailto:jhlu@iss.ac.cn) (J. Lü), [kmurali@annauniv.edu](mailto:kmurali@annauniv.edu) (K. Murali), [sudeshna@ims.res.in](mailto:sudeshna@ims.res.in) (S. Sinha).

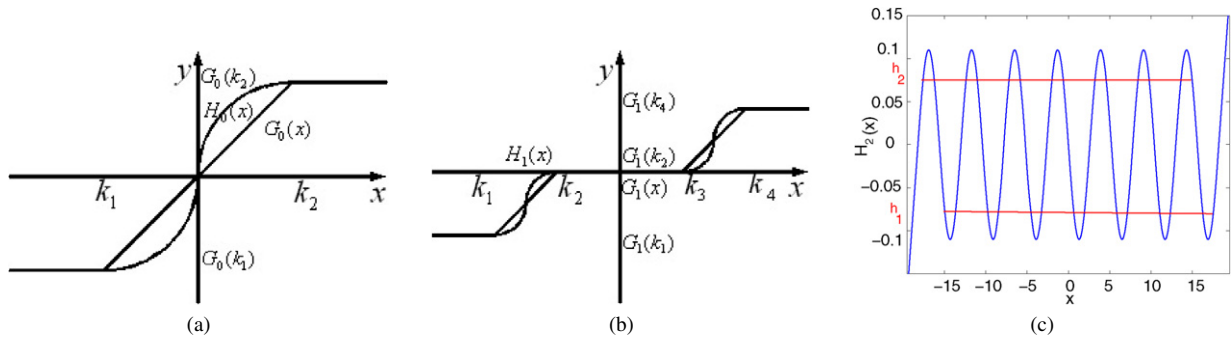


Fig. 1. (a) Threshold controllers  $G_0$  and  $H_0$ , where  $k_1$  and  $k_2$  are the lower and upper thresholds of  $x$ , respectively. (b) Threshold controllers  $G_1$  and  $H_1$ , where  $k_1, k_2, k_3$  and  $k_4$  are the lower threshold, middle thresholds and upper threshold of  $x$ , respectively. (c) Threshold controller  $H_2$ , where  $h_1$  and  $h_2$  are the lower and upper thresholds of the function of  $x$ , respectively.

plexity and more adjustability [9,15]. These properties indicate that multi-scroll chaos generation has a generally applied prospect in various chaos-based information technologies, such as encryption and secure communication [9,15]. In particular, multi-scroll chaotic attractors have many specific properties and functions. For example, Yalcin et al. applied the switching mechanism between two neighboring scrolls of a double-scroll attractor to create the true random bit [17]. Recently, Lü and Chen reviewed the main advances in theories, methods, implementations, and applications of multi-scroll chaos generation [15,17].

In the following, a novel threshold control method is introduced. We use a general jerk circuit and Chua’s circuit with sine nonlinearity as two representative examples to show the working principle of the threshold control approach [1,2,14,15, 17]. The controlled jerk circuit can generate various limit cycles and multi-scroll chaotic attractors by tuning the corresponding thresholds. The dynamic mechanism of the threshold control is then further investigated by analyzing the system dynamical behaviors. Furthermore, two novel circuit diagrams with threshold controllers are designed for the implementations of 1, 2, 3-scroll chaotic attractors. It tells us how to clip the practical current to generate the desired dynamical behaviors.

The rest of this Letter is organized as follows. In Section 2, a novel threshold control method is presented for creating multi-scroll chaotic attractors and two simple examples are then given. The dynamic mechanism of threshold control is then further investigated in Section 3. The novel circuit diagram with threshold controllers is then designed for the verifications of 1, 2, 3-scroll chaotic attractors in Section 4. Conclusions are drawn in Section 5.

## 2. A typical threshold control approach

To begin with, consider a general  $n$ -dimensional controlled system, which is described by

$$\dot{\mathbf{X}} = \mathbf{F}(\mathbf{X}, t) + \mathbf{H}(\mathbf{X}), \tag{1}$$

where  $\mathbf{X} = (x_1, x_2, \dots, x_n)^T \in \mathbf{R}^n$  is the state vector,  $\dot{\mathbf{X}} = \mathbf{F}(\mathbf{X}, t)$  is the original dynamical system, and  $\mathbf{H}(\mathbf{X})$  is a feedback threshold controller. The main working principle of this threshold controller is summarized as follows: when the vec-

tor function  $\varphi(\mathbf{X})$  exceeds a given threshold value  $h_0$ , then the controller is triggered and reset to vector  $\mathbf{X}^*$ , where  $\varphi(\mathbf{X})$  and  $\mathbf{X}^*$  are the input and output of the threshold controller  $\mathbf{H}(\mathbf{X})$ , respectively.

More detailedly, the threshold controller  $\mathbf{H}(\mathbf{X})$  depends on the original dynamical system  $\dot{\mathbf{X}} = \mathbf{F}(\mathbf{X}, t)$ . That is, the threshold controller  $\mathbf{H}(\mathbf{X})$  is then designed based on the dynamical behaviors of the system  $\dot{\mathbf{X}} = \mathbf{F}(\mathbf{X}, t)$ . Since both  $\mathbf{F}(\mathbf{X}, t)$  and  $\mathbf{H}(\mathbf{X})$  have many different algebraic forms, it is very difficult to give a unified theoretical analysis for the threshold controller  $\mathbf{H}(\mathbf{X})$ . However, for some specific nonlinear threshold controllers, such as the piecewise-linear and triangular functions controllers, there are some fundamental design criteria described in the following.

It should be especially pointed out that the thresholding method is completely different from most of known approaches of multi-scroll chaos generation [6–21]. For example, the fundamental working principle of the saturated function series as shown in Fig. 3 in [12] is to generate the scrolls by using basic saturated circuit and then connect all scrolls together. However, the main idea of the thresholding method is to clip the linear or nonlinear functions, including input and output variables and their functions, to yield the desired states by thresholding. The essential differences are outlined as follows: (i) the saturated function series is linearly increased between the neighboring saturated plateaus as shown in Fig. 3 in [12], however, the threshold controller may be nonlinearly increased as shown in Figs. 1(a)–(b), periodically changed as shown in Fig. 1(c), or even aperiodically changed; (ii) the saturated function series has a similar stair forms as shown in Fig. 3 in [12], however, the threshold controller may be very different in function form as shown in Fig. 1; (iii) the saturated function series is based on the independent variables or their linear functions, however, the threshold controller may be based on any independent or attribute variables, or even their any functions. Therefore, the thresholding approach has more freedom and plasticity on the design of multi-scroll chaos generation.

Fig. 1(a) shows the threshold controllers  $G_0$  and  $H_0$ , where  $k_1$  and  $k_2$  are the lower and upper thresholds of  $x$ , respectively. According to Fig. 1(a), when  $x \geq k_2$ , the threshold controller is triggered and then reset  $G_0(x)$  (or  $H_0(x)$ ) to  $G_0(k_2)$  (or  $H_0(k_2)$ ); when  $x \leq k_1$ , the threshold controller is triggered and

reset  $G_0(x)$  (or  $H_0(x)$ ) to  $G_0(k_1)$  (or  $H_0(k_1)$ ). Fig. 1(b) displays the threshold controllers  $G_1$  and  $H_1$  of  $x$ , where  $k_1, k_2, k_3$ , and  $k_4$  are the lower threshold, inner thresholds and upper threshold, respectively. Hereafter, the region  $[k_2, k_3]$  is called the inner threshold plateau. From Fig. 1(b), when  $x \geq k_4$ , the threshold controller is triggered and then reset  $G_1(x)$  (or  $H_1(x)$ ) to  $G_1(k_2)$  (or  $H_1(k_2)$ ); when  $x \leq k_1$ , the threshold controller is triggered and reset  $G_1(x)$  (or  $H_1(x)$ ) to  $G_1(k_1)$  (or  $H_1(k_1)$ ); when  $k_2 \leq x \leq k_3$ , the threshold controller is triggered and then reset  $G_1(x)$  (or  $H_1(x)$ ) to  $G_1(k_2)$  (or  $H_1(k_2)$ ). Fig. 1(c) shows the threshold controller  $H_2$ , where  $k_1$  and  $k_2$  are the lower and upper thresholds of the function of  $x$ , respectively. According to Fig. 1(c), when  $|x| \leq 18.2$  and  $H_2(x) \leq h_1$  (or  $H_2(x) \geq h_2$ ), the threshold controller is triggered and then reset  $H_2(x)$  to  $h_1$  (or  $h_2$ ).

In fact, the working principle of threshold controller is very simple. That is, the threshold controller appropriately clips linear or nonlinear functions to yield the desired states. In the following, we use a general jerk circuit as an example to show the detailed working principle of the above threshold controller [14,15,21]. A general jerk circuit is described by

$$\ddot{x} + c\dot{x} + bx + ax = G(x), \tag{2}$$

where  $a, b, c$  are real parameters,  $G(x)$  is a nonlinear threshold function,  $\dot{x} = \frac{dx}{dt}$  is the velocity,  $\ddot{x} = \frac{d^2x}{dt^2}$  is the acceleration,  $\dddot{x} = \frac{d^3x}{dt^3}$  is the jerk (or the changing rate of the acceleration by mechanical means),  $\tau = \frac{t}{R_0C_0}$ , in which  $\frac{1}{R_0C_0}$  is the transformation factor of the time scale, and also the integral constant of the integrator. Linz and Sprott studied the dynamical behaviors of some simple jerk circuits [18]. The chaos generation conditions of system parameters  $a, b, c$  will be further investigated in Section 3. For more detailed dynamical behaviors of system (2), please refer to [14,15,21] and references therein.

It is well known that system (2) is easy to be implemented by using the op-amps and diodes. Moreover, the threshold function  $G(x)$  has many different algebraic forms, such as step function, hysteresis function, saturated function, and even any functions by cutting the tails that exceed the given threshold values. For simplification,  $G_0(x; k_1, k_2)$  is described by

$$G_0(x; k_1, k_2) = \begin{cases} k_2, & \text{if } x > k_2, \\ x, & \text{if } k_1 \leq x \leq k_2, \\ k_1, & \text{if } x < k_1, \end{cases} \tag{3}$$

where  $k_2 > k_1$  and  $k_1, k_2$  are the lower and upper thresholds, respectively. Fig. 1(a) shows the threshold function  $G_0(x)$ , which can drive system (2) to create various limit cycles, single-scroll and double-scroll chaotic attractors by tuning the thresholds of controller  $G_0(x)$ .

System (2) with threshold controller (3) can generate various complex dynamical behaviors by tuning the thresholds  $k_1$  and  $k_2$  for fixed parameters  $a, b, c$ . When  $a = 0.38, b = 0.6, c = 0.35, k_1 = -1$ , some representative dynamical behaviors are listed below: (i) 2-cycle for  $0.15 \leq k_2 < 0.22$ ; (ii) 4-cycle for  $0.09 < k_2 < 0.15$ ; (iii) 8-cycle for  $k_2 \approx 0.08$ ; (iv) 3-cycle for  $0.297 \leq k_2 < 0.31$ ; (v) 6-cycle for  $k_2 \approx 0.32$ ; (vi) chaos for  $0.254 < k_2 < 0.296$  and  $0.4 < k_2 < 0.58$ ; (vii) 2-cycle for

$0.59 < k_2 < 0.64$ . These regions of parameter  $k_2$  are attained by carefully theoretical analysis and numerical calculation [1]. The more detailedly dynamical behaviors of system (2) with (3) are then further studied by using numerical calculation and theoretical analysis in Section 3.

To create the multi-scroll chaotic attractors from (2), one needs to set more thresholds. That is, one needs to carefully clip the threshold function into multiple segments. Consider a more general case,  $G_1(x; k_1, k_2, k_3, k_4)$  is then given by

$$G_1(x; k_1, k_2, k_3, k_4) = \begin{cases} k_4 - k_3, & \text{if } x > k_4, \\ x - k_3, & \text{if } k_3 \leq x \leq k_4, \\ 0, & \text{if } k_2 < x < k_3, \\ x - k_2, & \text{if } k_1 \leq x \leq k_2, \\ k_1 - k_2, & \text{if } x < k_1, \end{cases} \tag{4}$$

where  $k_1 < k_2 < k_3 < k_4$  and  $k_1, k_2, k_3, k_4$  are the lower, middle-left, middle-right and upper thresholds, respectively. Fig. 1(b) shows the threshold controller  $G_1(x)$ , which can drive system (4) to generate various limit cycles and 1, 2, 3-scroll chaotic attractors.

System (2) with threshold controller (4) can create various complex dynamical behaviors by tuning the thresholds  $k_1, k_2, k_3, k_4$  for fixed parameters  $a, b, c$ . When  $a = 0.38, b = 0.6, c = 0.35, k_1 = -2, k_2 = -k_3$  and  $k_4 = 2$ , some representative dynamical behaviors are outlined as follows: (i) 1-cycle for  $0.1 \leq k_3 - k_2 < 0.4$ ; (ii) 2-cycle for  $0.44 \leq k_3 - k_2 < 0.52$ ; (iii) 4-cycle for  $0.54 \leq k_3 - k_2 < 0.55$ ; (iv) 3-scroll chaotic attractor for  $1.2 \leq k_3 - k_2 < 2.0$ . The above regions of parameter  $(k_3 - k_2)$  are obtained by using carefully theoretical analysis and numerical calculation [1]. And the more detailedly dynamical behaviors of system (2) with (4) are further investigated via numerical calculation and theoretical analysis in Section 3.

Moreover, the threshold controller has many different algebraic forms. This is because the threshold controller may arbitrarily clip the independent and attributive variables and their functions to create a desired multi-scroll attractor. To clarify the diversity and plasticity of the threshold controller, one more example is then given in the following. Tang et al. introduced sine function into Chua's circuit for generating multi-scroll chaotic attractors [17], which is described by

$$\begin{cases} \dot{x} = \mu(y - H(x)), \\ \dot{y} = x - y + z, \\ \dot{z} = -vy, \end{cases}$$

and

$$H(x) = \begin{cases} \frac{b_1\pi}{2a_1}(x - 2a_1c_1), & x \geq 2a_1c_1, \\ -b_1 \sin(\frac{\pi x}{2a_1} + d_1), & |x| < 2a_1c_1, \\ \frac{b_1\pi}{2a_1}(x + 2a_1c_1), & x \leq -2a_1c_1, \end{cases}$$

where  $\mu, v, a_1, b_1, c_1, d_1$  are real parameters. When  $\mu = 10.814, v = 14.0, a_1 = 1.3, b_1 = 0.11, c_1 = 7, d_1 = 0$ ,  $H(x)$  is shown in Fig. 1(c).

It should be especially pointed out that the thresholding approach is very different from most of traditional chaoticification methods since there is no parameter perturbation in the controlled system. It only needs to clip the given threshold function by prescribed thresholds. The essence of thresholding approach

is to slightly limit the dynamic range of original dynamical system by snipping the state variables or their functions. Since a chaotic attractor has many temporary patterns, such as unstable periodic orbits, we can clip chaos to the desired dynamical behaviors by using suitable threshold controller. Moreover, the thresholding method can also be employed to generate various multi-scroll chaotic attractors by introducing appropriate thresholds in the controller.

### 3. Dynamic mechanisms of the threshold controllers $G_0(x)$ and $G_1(x)$

In this section, the dynamic mechanisms of the threshold controllers  $G_0(x)$  and  $G_1(x)$  are then further investigated.

#### 3.1. System (2) with the threshold controller (3)

System (2) with the threshold controller (3) is given by

$$\ddot{x} + c\dot{x} + b\dot{x} + ax = G_0(x). \tag{5}$$

Then system (5) can be divided into three different subspaces:  $V_1 = \{\mathbf{X} \mid x \geq k_2\}$ ,  $V_2 = \{\mathbf{X} \mid k_1 \leq x \leq k_2\}$ ,  $V_3 = \{\mathbf{X} \mid x \leq k_1\}$ , where  $\mathbf{X} = (x, \dot{x}, \ddot{x})^T \in \mathbf{R}^3$ . Under the coordinate transformation  $(x, \dot{x}, \ddot{x}) \rightarrow (-x, -\dot{x}, -\ddot{x})$ , system (5) has a natural symmetry for  $k_1 = -k_2$ . Moreover, system (5) is dissipative in each subspace for  $\frac{\partial \dot{x}}{\partial x} + \frac{\partial \ddot{x}}{\partial \dot{x}} + \frac{\partial \ddot{\ddot{x}}}{\partial \ddot{x}} = -c < 0$ .

If  $\mathbf{X} \in V_1, V_3$ , system (5) becomes

$$\ddot{\tilde{x}} + c\dot{\tilde{x}} + b\dot{\tilde{x}} + a\tilde{x} = 0, \tag{6}$$

where  $(\tilde{x}, \dot{\tilde{x}}, \ddot{\tilde{x}})^T = (x - \frac{k_2}{a}, \dot{x}, \ddot{x})^T$  for  $\mathbf{X} \in V_1$  and  $(\tilde{x}, \dot{\tilde{x}}, \ddot{\tilde{x}})^T = (x - \frac{k_1}{a}, \dot{x}, \ddot{x})^T$  for  $\mathbf{X} \in V_3$ .

The eigenvalues of system (6) are then given by

$$\lambda_1 = -\frac{c}{3} + \sqrt[3]{-\frac{q}{2} + \sqrt{\Delta}} + \sqrt[3]{-\frac{q}{2} - \sqrt{\Delta}}, \tag{7}$$

and

$$\begin{aligned} \lambda_{2,3} &= -\frac{c}{3} - \frac{1}{2} \left( \sqrt[3]{-\frac{q}{2} + \sqrt{\Delta}} + \sqrt[3]{-\frac{q}{2} - \sqrt{\Delta}} \right) \\ &\quad \pm \frac{\sqrt{3}}{2} i \left( \sqrt[3]{-\frac{q}{2} + \sqrt{\Delta}} - \sqrt[3]{-\frac{q}{2} - \sqrt{\Delta}} \right) \\ &\equiv \alpha \pm \beta i, \end{aligned} \tag{8}$$

where  $\Delta = \frac{ac^3}{27} - \frac{b^2c^2}{108} - \frac{abc}{6} + \frac{b^3}{27} + \frac{a^2}{4}$ ,  $p = b - \frac{1}{3}c^2$ , and  $q = \frac{2}{27}c^3 - \frac{1}{3}bc + a$ .

Our numerical simulations reveal that system (5) can generate chaotic attractors under the conditions of  $\lambda_1 < 0, \alpha > 0, \beta \neq 0$ . Therefore, the solution of system (6) is given by

$$\tilde{x}(t) = A_1 e^{\lambda_1 t} + e^{\alpha t} (A_2 \cos(\beta t) + A_3 \sin(\beta t)), \tag{9}$$

where  $A_1 = ((\alpha^2 + \beta^2)\tilde{x}(0) - 2\alpha\dot{\tilde{x}}(0) + \ddot{\tilde{x}}(0))/((\lambda_1 - \alpha)^2 + \beta^2)$ ,  $A_2 = ((\lambda_1^2 - 2\alpha\lambda_1)\tilde{x}(0) + 2\alpha\dot{\tilde{x}}(0) - \ddot{\tilde{x}}(0))/((\lambda_1 - \alpha)^2 + \beta^2)$ ,  $A_3 = ((\lambda_1\alpha^2 - \lambda_1\beta^2 - \lambda_1^2\alpha)\tilde{x}(0) - (\beta^2 - \alpha^2 + \lambda_1^2)\dot{\tilde{x}}(0) + (\alpha - \lambda_1)\ddot{\tilde{x}}(0))/(\beta[(\lambda_1 - \alpha)^2 + \beta^2])$ .

Similarly, if  $\mathbf{X} \in V_2$ , then system (5) is described by

$$\ddot{x} + c\dot{x} + b\dot{x} + (a - 1)x = 0, \tag{10}$$

and its solution is given by

$$x(t) = \bar{A}_1 e^{\bar{\lambda}_1 t} + e^{\bar{\alpha} t} (\bar{A}_2 \cos(\bar{\beta} t) + \bar{A}_3 \sin(\bar{\beta} t)), \tag{11}$$

where  $\bar{A}_1 = ((\bar{\alpha}^2 + \bar{\beta}^2)x(0) - 2\bar{\alpha}y(0) + z(0))/((\bar{\lambda}_1 - \bar{\alpha})^2 + \bar{\beta}^2)$ ,  $\bar{A}_2 = ((\bar{\lambda}_1^2 - 2\bar{\alpha}\bar{\lambda}_1)x(0) + 2\bar{\alpha}y(0) - z(0))/((\bar{\lambda}_1 - \bar{\alpha})^2 + \bar{\beta}^2)$ ,  $\bar{A}_3 = ((\bar{\lambda}_1\bar{\alpha}^2 - \bar{\lambda}_1\bar{\beta}^2 - \bar{\lambda}_1^2\bar{\alpha})x(0) - (\bar{\beta}^2 - \bar{\alpha}^2 + \bar{\lambda}_1^2)y(0) + (\bar{\alpha} - \bar{\lambda}_1)z(0))/(\bar{\beta}[(\bar{\lambda}_1 - \bar{\alpha})^2 + \bar{\beta}^2])$ , in which parameters  $\bar{\alpha}, \bar{\beta}, \bar{\lambda}_1$  are similarly defined by (7) and (8) with  $a$  replaced by  $(a - 1)$ .

Based on the above theoretical analysis, the dynamical behaviors of system (5) are completely determined by (9) and (11). In essence, the function of threshold controller  $G_0$  is to alternatively switch the dynamics between (9) and (11). Especially, the two thresholds  $k_1, k_2$  control the displacement transformation of the state variable  $x$ . System (5) can create various limit cycles, single-scroll and double-scroll chaotic attractors via tuning the thresholds  $k_1, k_2$  of  $G_0$ .

#### 3.2. System (2) with the threshold controller (4)

System (2) with the threshold controller (4) is given by

$$\ddot{x} + c\dot{x} + b\dot{x} + ax = G_1(x). \tag{12}$$

Thus system (12) can be divided into five different subspaces as follows:  $V_1 = \{\mathbf{X} \mid x \geq k_4\}$ ,  $V_2 = \{\mathbf{X} \mid k_3 \leq x \leq k_4\}$ ,  $V_3 = \{\mathbf{X} \mid k_2 \leq x \leq k_3\}$ ,  $V_4 = \{\mathbf{X} \mid k_1 \leq x \leq k_2\}$ ,  $V_5 = \{\mathbf{X} \mid x \leq k_1\}$ , where  $\mathbf{X} = (x, \dot{x}, \ddot{x})^T \in \mathbf{R}^3$ . System (12) has a natural symmetry for  $k_1 = -k_4$  and  $k_2 = -k_3$  under the coordinate transformation  $(x, \dot{x}, \ddot{x}) \rightarrow (-x, -\dot{x}, -\ddot{x})$ . Moreover, system (12) is dissipative in each subspace for  $c > 0$ .

When  $\mathbf{X} \in V_1, V_3, V_5$ , system (12) becomes (6), where  $(\tilde{x}, \dot{\tilde{x}}, \ddot{\tilde{x}})^T = (x - \frac{k_4 - k_3}{a}, \dot{x}, \ddot{x})^T$  for  $\mathbf{X} \in V_1$ ,  $(\tilde{x}, \dot{\tilde{x}}, \ddot{\tilde{x}})^T = (x, \dot{x}, \ddot{x})^T$  for  $\mathbf{X} \in V_3$ , and  $(\tilde{x}, \dot{\tilde{x}}, \ddot{\tilde{x}})^T = (x - \frac{k_1 - k_2}{a}, \dot{x}, \ddot{x})^T$  for  $\mathbf{X} \in V_5$ .

When  $\mathbf{X} \in V_2, V_4$ , the system (12) becomes

$$\ddot{\hat{x}} + c\dot{\hat{x}} + b\dot{\hat{x}} + (a - 1)\hat{x} = 0, \tag{13}$$

where  $(\hat{x}, \dot{\hat{x}}, \ddot{\hat{x}})^T = (x + \frac{k_3}{a}, \dot{x}, \ddot{x})^T$  for  $\mathbf{X} \in V_2$  and  $(\hat{x}, \dot{\hat{x}}, \ddot{\hat{x}})^T = (x + \frac{k_2}{a}, \dot{x}, \ddot{x})^T$  for  $\mathbf{X} \in V_4$ .

Then the solution of system (13) is also given by (11) since (13) has the same algebraic form with (11). Our theoretical

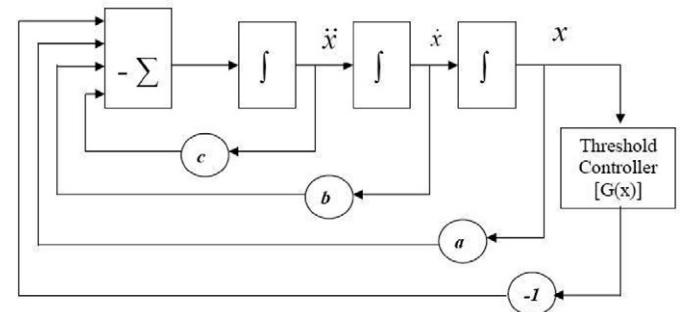


Fig. 2. The diagrammatic sketch of the structure for the proposed threshold control system (12).



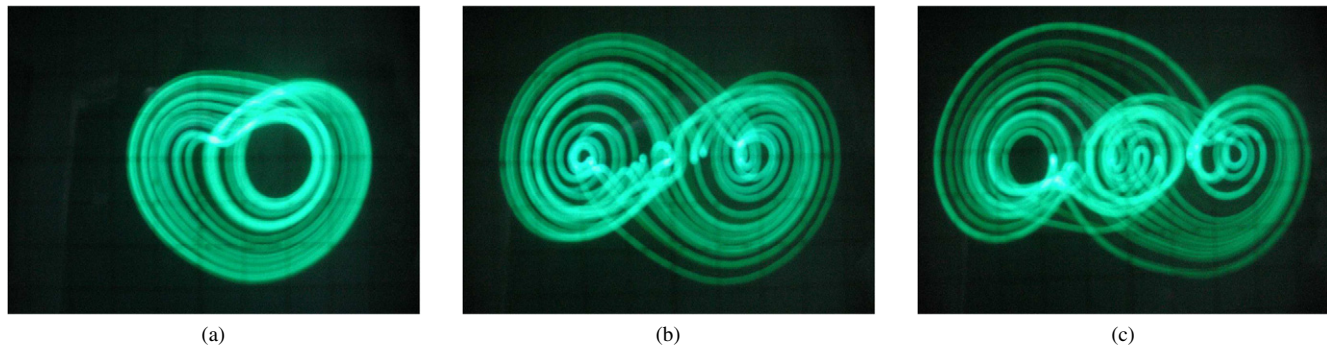


Fig. 3. Phase portraits of the experimental observations for  $n$ -scroll chaotic attractors in the  $x-\dot{x}$  plane. (a)  $n = 1$ , (b)  $n = 2$ , (c)  $n = 3$ .

analysis also indicates that the dynamical behaviors of system (12) are completely determined by (9) and (11). In fact, the main function of threshold controller  $G_1$  is to alternatively switch the dynamics between (9) and (11). In particular, the four thresholds  $k_1, k_2, k_3, k_4$  control the displacement transformation of state variable  $x$ . System (12) can create various limit cycles and 1, 2, 3-scroll chaotic attractors via tuning the thresholds  $k_1, k_2, k_3, k_4$  of  $G_1$ .

#### 4. Circuit implementation

This section shows how to clip the practical current to generate the desired dynamical behaviors based on the designed threshold controllers. The basic design idea is outlined as follows.

Fig. 2 displays the diagrammatic sketch of the structure for the proposed threshold control system (12), which depicts the basic procedure of the current realization. As a straightforward technique, three lossless integrators are cascaded and a summing amplifier is employed to form a feedback loop. A threshold controller is then utilized to realize the function  $G(x)$ . Fig. 3(a) shows the  $(x-\dot{x})$  plane projection of a 1-scroll chaotic attractor, where the threshold control voltage levels are  $B1 = 0.3$  V and  $B2 = -0.7$  V. Moreover, if one slightly adjusts the threshold control voltage level  $B2$  to  $-0.3$  V, then the circuit exhibits a typical 2-scroll chaotic attractor as shown in Fig. 3(b). When the threshold control voltage levels of the batteries are fixed at  $B1 = +1.3$  V,  $B2 = -1.3$  V,  $B3 = -0.3$  V and  $B4 = +0.3$  V, a typical 3-scroll chaotic attractor is observed as shown in Fig. 3(c). Finally, our circuit experiments show that all circuit parameters are rather robust against small perturbation or noise.

#### 5. Conclusions

This Letter has introduced a systematic threshold control approach for generating multi-scroll chaotic attractors. We use the general jerk circuit and Chua's circuit with sine nonlinearity as two representative examples to show the main working principle of the threshold control method. The dynamic mechanism of this threshold control approach is then further explored by analyzing the system dynamical behaviors of the general controlled jerk circuit. The controlled jerk system can generate various limit cycles and multi-scroll chaotic attractors by tuning the cor-

responding thresholds. Moreover, this thresholding approach is very effective and simple since one only needs to monitor the threshold variables or their functions and then reset them if they exceed the given thresholds. Finally, two novel circuit diagrams with threshold controllers are designed for the implementations of 1, 2, 3-scroll chaotic attractors. The high complexity, adjustability, and plasticity provide a general applied prospect for multi-scroll chaotic attractors in chaos-based information and communication systems. Recently, we have successfully realized the voice encryption and communication by using multi-scroll chaotic attractors and digital signal processing. Detailed results will be reported in the near future.

#### Acknowledgements

This work was supported by the National Natural Science Foundation of China under Grants Nos. 60772158 and 60221301, the Scientific Research Startup Special Foundation on Excellent PhD Thesis and Presidential Award of Chinese Academy of Sciences (CAS), the Important Direction Project of Knowledge Innovation Program of CAS under Grant No. KJCX3-SYW-S01, and the 973 Program of China under Grant No. 2007CB310805.

#### References

- [1] G. Chen, J. Lü, Dynamics of the Lorenz System Family: Analysis, Control and Synchronization, Science Press, Beijing, 2003 (in Chinese).
- [2] M. Lakshmanan, K. Murali, Chaos in Nonlinear Oscillators: Controlling and Synchronization, World Scientific, Singapore, 1996.
- [3] S. Sinha, W.L. Ditto, Phys. Rev. Lett. 81 (1998) 2156.
- [4] K. Murali, S. Sinha, Phys. Rev. E 68 (2003) 016210.
- [5] S. Sinha, D. Biswas, Phys. Rev. Lett. 71 (1993) 2010.
- [6] J.A.K. Suykens, J. Vandewalle, IEEE Trans. Circuits Syst. I 40 (1993) 861.
- [7] J. Lü, T. Zhou, G. Chen, X. Yang, Chaos 12 (2002) 344.
- [8] J. Lü, X. Yu, G. Chen, IEEE Trans. Circuits Syst. I 50 (2003) 198.
- [9] M.E. Yalcin, J.A.K. Suykens, J.P.L. Vandewalle, Cellular Neural Networks, Multi-Scroll Chaos and Synchronization, World Scientific, Singapore, 2005.
- [10] J. Lü, F. Han, X. Yu, G. Chen, Automatica 40 (2004) 1677.
- [11] J. Lü, G. Chen, D. Cheng, S. Čelikovský, Int. J. Bifur. Chaos Appl. Sci. Eng. 12 (2002) 2917.
- [12] J. Lü, G. Chen, X. Yu, H. Leung, IEEE Trans. Circuits Syst. I 51 (2004) 2476.
- [13] J. Lü, S.M. Yu, H. Leung, G. Chen, IEEE Trans. Circuits Syst. I 53 (2006) 149.

- [14] S.M. Yu, J. Lü, H. Leung, G. Chen, *IEEE Trans. Circuits Syst. I* 52 (2005) 1459.
- [15] J. Lü, G. Chen, *Int. J. Bifur. Chaos Appl. Sci. Eng.* 16 (2006) 775.
- [16] M.E. Yalcin, J.A.K. Suykens, J. Vandewalle, S. Ozoguz, *Int. J. Bifur. Chaos Appl. Sci. Eng.* 12 (2002) 23.
- [17] J. Lü, G. Chen, *Int. J. Bifur. Chaos Appl. Sci. Eng.* 12 (2002) 659.
- [18] S.J. Linz, J.C. Sprott, *Phys. Lett. A* 259 (1999) 240.
- [19] S.M. Yu, J. Lü, G. Chen, *Chaos* 17 (2007) 013118.
- [20] S.M. Yu, J. Lü, W.K.S. Tang, G. Chen, *Phys. Lett. A* 364 (3) (2007) 244.
- [21] S.M. Yu, J. Lü, W.K.S. Tang, G. Chen, *Chaos* 16 (2006) 033126.